Yao et al. Journal of Translational Medicine (2025) 23:284
https://doi.org/10.1186/s12967-025-06240-9

Journal of Translational Medicine

RESEARCH Open Access

Melanophilin inhibit the growth and lymph node metastasis of triple negative breast cancer via the NONO-SPHK1-S1P axis

Xing Yao[1†], Tan Yuen[3†], Chen Qingchuan[4†], Zhang Jianjun[3*], Liu Yefu[2*] and Sun Shulan[1*]

Abstract

Background Triple negative breast cancer (TNBC) is the most aggressive breast cancer subtype with the worst prognosis, and there are no targeted treatments available. TNBC patients are more likely to develop metastases and relapse than patients with other breast cancer subtypes. Lymph node metastasis is the first sign of metastatic spread. We aimed to characterize the mechanism of lymph node metastasis in TNBC to provide a new strategy for the treatment of TNBC.

Methods Gene Expression Omnibus (GEO) TNBC database was utilized to screen for genes related to N staging. Screening the downstream target of Melanophilin (MLPH) in TNBC through RNA sequencing (RNA seq) analysis. Protein mass spectrometry was utilized to analyze the protein which interacts with MLPH, and RNA binding protein immunoprecipitation and quantitative real-time PCR (RIP qPCR) were utilized to verify the regulation of sphingosine kinase 1 (SPHK1) expression by MLPH through Non-POU domain-containing octamer-binding protein (NONO). Cell functional assays and in vivo models experiments further confirmed the effects of MLPH on proliferation and lymph node metastasis of TNBC through the SPHK1-S1P axis.

Results MLPH is downregulated in TNBC and inhibits tumor growth and lymph node metastasis though the MLPH-NONO-SPHK1-S1P pathway. NONO was identified as an essential factor involved in SPHK1 mRNA splicing. MLPH interacts with NONO to inhibit SPHK1 mRNA splicing of SPHK1, which reduces the content of S1P, thereby inhibiting growth and lymph node metastasis in TNBC.

Conclusions This study preliminarily elucidated a mechanism underlying lymph node metastasis in TNBC and identified the role of the MLPH-NONO-SPHK1-S1P axis in regulating proliferation and lymph node metastasis in TNBC. These findings may help design strategies for predicting and treating metastasis in TNBC.

Keywords MLPH, TNBC, Lymph node metastasis

†Xing Yao, Tan Yuen and Chen Qingchuan are Co-first authors.

*Correspondence:
Zhang Jianjun
zhangjianjun@cancerhosp-ln-cmu.com
Liu Yefu
97902153@cmu.edu.cn
Sun Shulan
sunshulan@cancerhosp-ln-cmu.com

[1]Central Laboratory, Cancer Hospital of Dalian University of Technology (Cancer Hospital of China Medical University, Liaoning Cancer Hospital & Institute), Shenyang, Liaoning 110042, P. R. China
[2]Department of Hepatopancreatobiliary Surgery, Liaoning Cancer Hospital and Institute, Shenyang, Liaoning 110042, P. R. China
[3]Department of Gastric Surgery, Cancer Hospital of Dalian University of Technology (Cancer Hospital of China Medical University, Liaoning Cancer Hospital & Institute), Shenyang, Liaoning 110042, P. R. China
[4]Department of Gastric Surgery, School of Medicine, Sichuan Cancer Hospital, University of Electronic Science and Technology of China, Chengdu, China

Introduction

Breast cancer metastasis is the main cause of death among women worldwide, and lymph node metastasis is the most common form of breast cancer metastasis, as well as an important criterion to define the stage of breast cancer [1]. Triple negative breast cancer(ER, PR, and HER2 negative, TNBC) is the most aggressive subtype, accounting for 10 -24% of all breast cancer cases [2, 3]. There are no effective targeted therapies for TNBC, and identifying new biomarkers and specific targets is thus considered top priority in both theoretical research and clinical practice.

Melanophilin (MLPH) forms a ternary complex with the small Ras-related GTPase Rab27A in its GTP-bound form and the motor protein myosin Va. The complex interacts with the actin cytoskeleton and is essential for the maintenance of a dispersed state of melanosomes [4, 5]. Increased expression of MLPH in rectal cancer patients is associated with poor responses to preoperative radiotherapy and chemotherapy and low survival rates [6]. Consistently, O-GlcNAcylation of MLPH enhances radiation resistance in glioblastoma by suppressing TRIM21-mediated ubiquitination [7]. However, the role of MLPH in TNBC has not been well studied.

The multifunctional bioactive lipid mediator sphingosine-1-phosphate (S1P) promotes tumor cell proliferation, migration, invasion, angiogenesis, and drug resistance, and has been identified as a key regulatory molecule in cancer [8–10]. S1P is produced in cells by two types of sphingosine kinases (SPHK1 and SPHK2) and regulates many functions by interacting with and signaling through five G protein coupled receptor families. S1P produced by SPHK2 is localized in the nucleus and inhibits histone deacetylase (HDAC1/2) activity, which increases gene transcription activity [11]. By contrast, S1P produced by SPHK1 is mainly located within the cell or secreted into the extracellular matrix [8, 12]. Inhibition of SPHK1 activity decreases the growth of primary mammary tumors and suppresses lung metastasis [13–15]. However, the effect of the SPHK1-S1P axis on lymph node metastasis in TNBC remains unknown.

mRNAs undergo several post-transcriptional regulatory events, including splicing, transport, and modification that are prerequisites for translation into proteins. These processes are governed by the action of RNA-binding proteins (RBPs), which are related to many human diseases [16, 17]. Non-POU domain-containing octamer-binding protein (NONO) is an RBP that is involved in different physiological and pathological processes, and its function is regulated by different mechanisms [18, 19]. The circular RNA circ-hnRNPU downregulates glycosyl transferases and the parental gene hnRNPU by repressing nuclear NONO-mediated c-Myc transactivation or cytoplasmic NONO-facilitated mRNA stability to inhibit N- and O-glycosylation, growth, invasion, and metastasis of gastric cancer cells [20]. Loss of NONO induces intron retention of glutathione peroxidase 1(GPX1) and cellular communication network factor 1(CCN1) to impair redox homeostasis, apoptosis, and invasion in glioblastoma multiforme [21]. Modulation of EGFR and STAT3 stabilization by NONO exert oncogenic effects and are associated with chemotherapy resistance and poor prognosis in patients with TNBC [22, 23]. mechanisms underlying the regulation of SPHK1 by NONO remain unclear.

In this study, we found MLPH is downregulated in TNBC and inhibits tumor growth and lymph node metastasis though the MLPH-NONO-SPHK1-S1P pathway. NONO was identified as an essential factor involved in SPHK1 mRNA splicing. MLPH interacts with NONO to inhibit mRNA splicing of SPHK1, which reduces the content of S1P, thereby inhibiting growth and lymph node metastasis in TNBC. These data indicate that targeting the MLPH-NONO-SPHK1-S1P pathway could be a new strategy for the treatment of TNBC.

Materials and methods

Construction of weighted gene co-expression network analysis (WGCNA)

This article retrieved 11 TNBC-GEO databases, including GSE45498, GSE137356, GSE65194, GSE65212, GSE76275, GSE76124, GSE76274, GSE142102, GSE76250, GSE62931, and GSE135565. Based on the completeness of clinical information and annotation platforms, two GEO databases, GSE65194 ($N = 178$) and GSE76124 ($N = 198$), were ultimately selected. Excluding IDs with incomplete clinical information, a total of 214 TNBCs were included for WGCNA analysis.

Plasmid and lentiviral vector construction and transfection

MLPH-Lentivirus and MLPH RNAi-Lentivirus were purchased from GeneChem Company (Shanghai, China). 1×10^5 cells were infected with 2 μl of 1×10^9 TU lentivirus for 24 h and selected with 5 μg/ml puromycin.

Mass spectrometry analysis

Cells were collected into IP lysis buffer and the cell lysate was incubated on ice for 30 min and incubated with MLPH antibody-conjugated agarose beads with rotation at 4 C for 12 h. The binding protein was eluted into SDS loading buffer and analyzed by mass spectrometry.

RNA-seq analysis

Flag vector or Flag-MLPH was stably expressed in mammary adenocarcinoma MDA-MB-231 cells. The total RNA extractions were using the TRIzol (Invitrogen, USA). RNA-seq analysis was performed at Wuhan seqhealth Inc. (Wuhan, China).

Western blot and immunoprecipitation assay

Immunoprecipitation and western blot analyses have been described previously [24].

Reagents and antibodies

Antibodies against proteins were used in the experiments in follows and were purchased from protein tech, Wuhan China: MLPH (#10338-1-AP); SPHK1 (#10670-1-lg); NONO (#11058-1-AP); Actin (#66009-1-lg); LaminB1 (#12987-1-AP); β-Tubulin (#10068-1-AP); Flag and GAPDH (#66008-4-lg; #60004-1-lg).

Patient tissues and specimens

The present study was approved by the Ethics Committee of the Cancer Hospital of China Medical University. A total of 210 patients with primary breast cancer who did not receive any preoperative chemotherapy or radiotherapy in the period 2013–2015 were enrolled in this study. Ethical practices were followed throughout to ensure patient data confidentiality and compliance with the Declaration of Helsinki. Clinical stage was classified according to the eighth edition of the American Joint Committee on Cancer TNM criteria for breast cancer. The prognostic data of all patients were obtained by referring to medical records; data from patients with nontumor death were excluded. Disease-free survival (DFS) was defined as the time between surgery and the onset of local recurrence or distant metastasis. Overall survival (OS) was defined as the period from surgery to death.

Colony formation assay

5×10^2 Cells were cultured in 6-well plates until visible cell colonies were formed. The cells are fixed and stained, and the number of colonies was measured.

CCK8 assay

CCK8 reagent was added to incubate at 37 °C for 2 h, and the laser detection with the wavelength of 450 nm was used. The data was calculated according to the reagent instructions.

S1P detection assay

The level of intracellular and extracellular S1P was determined using a S1P enzyme-linked immunosorbent assay kit (ml038623, mlbio, China). Briefly, HS578T cells and MDA-MB-231 cells were seeded in 60-mm dishes and incubated in serum-free RPMI-1640 for 48 h. Then, the cells were harvested, and the levels of S1P were measured according to the manufacturer's instructions.

Transwell migration and invasion assay

To assess cell migration and invasion in vitro, MDA-MB-231 cells (1×10^5 cells in 100 µl Leibovitz's L-15 Medium without FBS) and HS578T cells (1×10^5 cells in 100 µl Dulbecco's Modified Eagle Medium without FBS) were placed in the top chamber of transwell migration chambers. In the cell invasion assay in vitro, the upper chamber of transwells was treated with 10% matrix gel, and the other steps were the same as above. The transwell migration and invasion assay used in this study has been described previously in detail [24].

Wound healing assay

A total of 2×10^6 MDA-MB-231 cells or HS578T cells stably transfected with the indicated constructs were seeded in six-well plates. The transwell migration assay used in this study has been described previously in detail [24].

RNA isolation and qRT-PCR

Total RNA isolation and qRT-PCR were carried out according to the protocol used in our previous study [24].

Immunohistochemical (IHC) staining

Paraffin sections cut from paraffin-embedded breast cancer tissues were dewaxed and rehydrated. IHC staining assay was used to detected the expression of MLPH in all tumor sections with the MLPH antibody. Then the nucleus was stained with hematoxylin (Maixin Biotechnology Co., Ltd). After hydration and transparent, the sections were sealed with neutral resins and photographed.

RNA binding protein immunoprecipitation (RIP)

RIP was performed using the EZ-Magna RIP RNA-Binding Protein Immunoprecipitation Kit (Merck Millipore; Burlington, MA, USA). In brief, cells were cross-linked with 1% formaldehyde and lysed with protease and RNase inhibitors. Magnetic beads preincubated with IgG or antibody specific for NONO were incubated with lysates at 4 °C overnight. Eluted RNAs were purified and detected with qPCR. Total RNA was regarded as the input control.

Cell adhesion

10 µg/ml collagen was coated in a 96 well plate at room temperature for 1 h and washed twice with serum-free culture medium. Spread 30,000 cells in the well plate and cultured for 2 h, wash with PBS three times, and detect the number of cells in the well plate with CCK8.

Animal models

All experiments involving mice were carried out in accordance with the National Institutes of Health Guide for the Care and Use of Laboratory Animals (NIH Publication No. 8023, revised 1978). All mice were maintained and bred at the Animal Center of China Medical University. Animal experiments were approved by the Animal

Center of China Medical University and Use Committees of China Medical University. For 4T1 cell footpad implantation model, 2×10^5 4T1-Flag or 4T1-Flag-MLPH cells were implanted subcutaneously into the footpad region of hind limb of 6 ~ 8-week-old female BALB/c mice. S1P (300 mg/kg of body weight, Sigma-Aldrich, #SML2709) in PBS (50 μl) was injected daily subcutaneously to the anterolateral side of mouse leg, right above the hind limb foot where 4T1 cells were implanted. The treatment was started from the 2nd week after tumor implantation. Ipsilateral pLNs tissues were sampled at day 25. The 2×10^6 stably transfected 4T1 cells were injected subcutaneously into 6 ~ 8-week-old female BALB/c mice. Tumor volume was measured once every 3 days. The calculation formula was tumor volume = π/6 × (L × W × H). Mice were killed after 30 days.

Statistical analysis

We used GraphPad Prism software for statistical analyses. Student's t-test (2-tailed) was applied to compare differences between two groups in repeated studies. The significance of differences in specimen data was determined with a chi-square test. $^{*}p < 0.05$ was considered statistically significant, and $^{**}p < 0.01$, $^{***}p < 0.001$ and $^{****}p < 0.0001$ were considered highly significant. The Kaplan–Meier method was used to generate survival curves.

Results

Gene expression information from 21,626 genes was extracted from two TNBC GEO datasets (GSE65194, GSE76124), and the expression of each gene was analyzed in 214 patient samples using ANOVA. The top 25% of genes (5407) was selected for subsequent WGCNA analysis. Cluster analysis using the clinicopathological factors age, T stage, N stage, M stage, and histological type was followed by calculation of the soft threshold (Fig. 1a). When the soft threshold was set at 3, the scale independent R2 value was 0.868 (Fig. 1b). Based on the soft threshold, 11 network modules were ultimately determined by hierarchical clustering of gene expression levels and the corresponding clinicopathological factors (Fig. 1c-f). The yellow module related to N stage was selected for further analysis (correlation coefficient: 0.18, Fig. 1d). The genes in the yellow module were selected for analysis, and the correlation between the two of the module membership and the significance of genes was 0.37 (Fig. 1f). Analysis of the relationships between genes in the yellow module by Cytoscape showed that, the higher the weight of the network in the module, the greater the representativeness effect. Application of the Maximal Clique Centrality (MCC) algorithm in the plug-in, identified the following ten key genes in the network: FOXA1, MLPH, TSPAN13, SPDEF, KIF16B, STARD10, AGR2, ARSG, C9orf152, and SLC4A8 (Fig. 1g).

To identify genes associated with lymph node metastasis in TNBC, we used the GEO database to measure the Recurrence free survival (RFS) of hub genes in the yellow module. Patients with low MLPH expression had a worse prognosis. Further analysis shows that compared with the patients without lymph node metastasis, low MLPH expression was more correlated with poor prognosis in patients with lymph node metastasis (Fig. 2a). The expression of the two other genes (FOXA1 and TSPAN13) analyzed was no significant difference in survival rates between patients with or without lymph node metastasis (Figure S1a and b). Analysis of the expression of MLPH in normal tissues and in different subtypes of breast cancer in The Cancer Genome Atlas (TCGA) and the Clinical Proteomic Tumor Analysis Consortium (CPTAC) databases showed that MLPH is downregulated in TNBC (Fig. 2b and c). In addition, analysis of 50 pairs of fresh frozen clinical samples of different subtypes of breast cancer tissues and paired adjacent nonneoplastic tissues showed that MLPH protein expression was higher in breast cancer than in non-tumor tissues (Figure S2a and b). MLPH expression was lower in TNBC than in other breast cancer subtypes (Fig. 2d and e). IHC staining assay and histopathological analysis of 129 breast cancer cases showed that MLPH expression was lower in TNBC (Fig. 2f and g), and MLPH was negatively correlated with metastasis in TNBC rather than other breast cancer subtypes (Fig. 2h). Kaplan Meier survival analysis showed that low MLPH levels were associated with poor overall survival and poor disease-free survival. Stratification of patients according to subtype of breast cancer showed that the association of low MLPH levels with poor overall survival and disease-free survival was more prominent in TNBC patients than in other tumor subtypes (Fig. 2i). These results indicate that MLPH is downregulated and negatively corelated with lymph node metastasis and poor survival in TNBC.

Detection of MLPH in different cell lines showed that MLPH expression was lower in TNBC cell lines than in other cancer cell lines (Fig. 3a). Next, we examined cell migration and invasion in cells from different subtypes of breast cancer using wound healing and transwell migration and invasion assays. The results showed that invasion and migration abilities were stronger in TNBC cells than other cell lines (Fig. 3b and c). These results indicate that the expression of MLPH may be related to the invasion and migration of breast cancer cells. To explore the role of MLPH in the occurrence and development of TNBC, we used HS578T cells and MDA-MB-231 cells stably expressing MLPH. Cells with MLPH overexpression showed significantly lower proliferation rates in vitro than the control (Fig. 3d and e). Colony formation

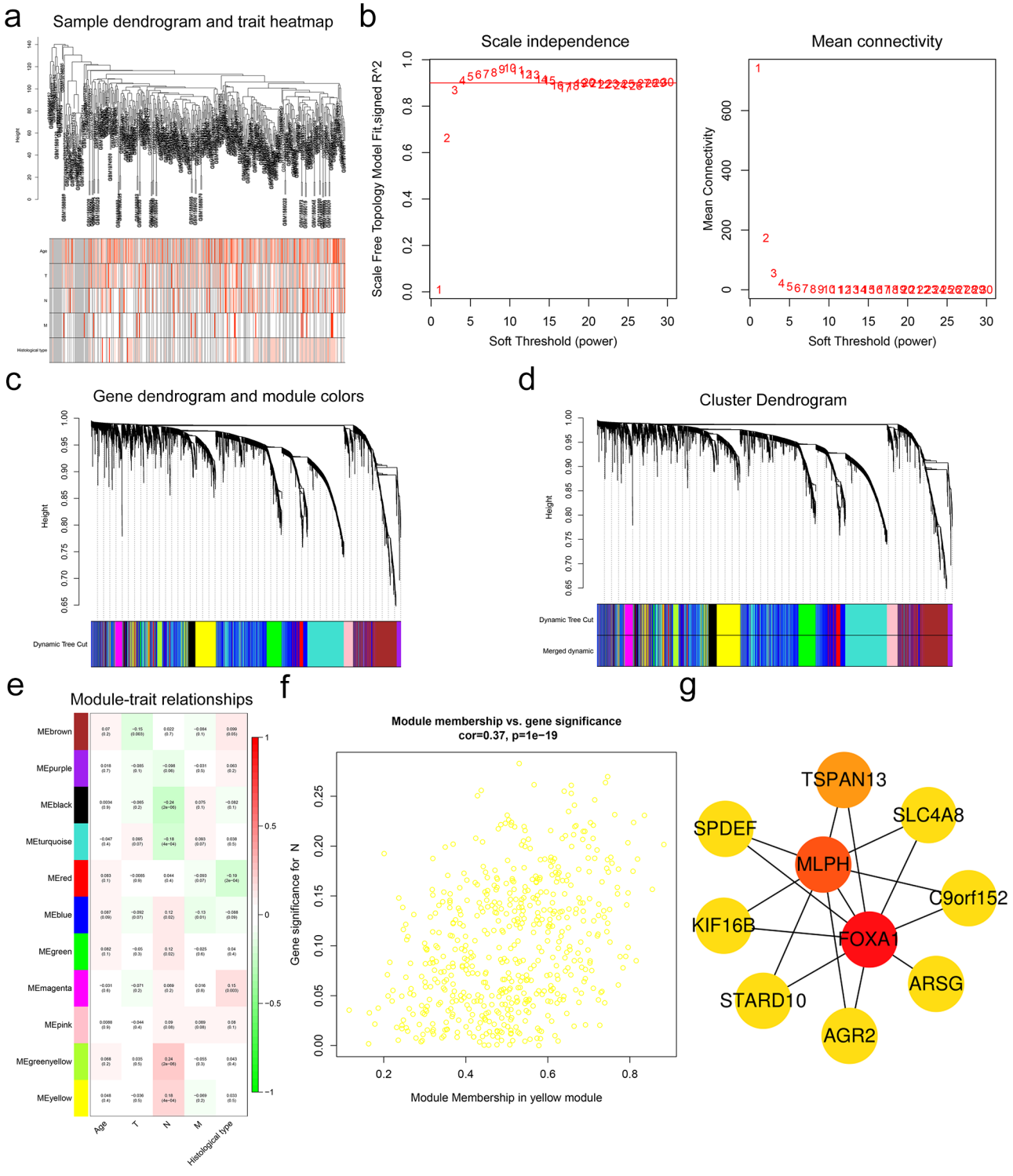

Fig. 1 Identification of the key gene MLPH related to lymph node metastasis in TNBC. **a**. Clustering dendrogram of the clinical traits. **b**. Calculation of the soft threshold by scale independence and mean connectivity. When the soft threshold was 3, the scale free topology fitting index R2 was 0.868. **c** and **d**. Clustering dendrogram of genes based on topological overlap. **e**. Heatmap of modules for gene-traits relationship. Red represents a positive correlation, and green represents a negative correlation. **f**. The correlation between yellow module membership and N staging was significant. The correlation coefficient was 0.37. **g**. Utilization of Cytoscape to visualize the relationship between genes in the yellow module. ten key genes were selected from the network using the Maximal Clique Centrality algorithm

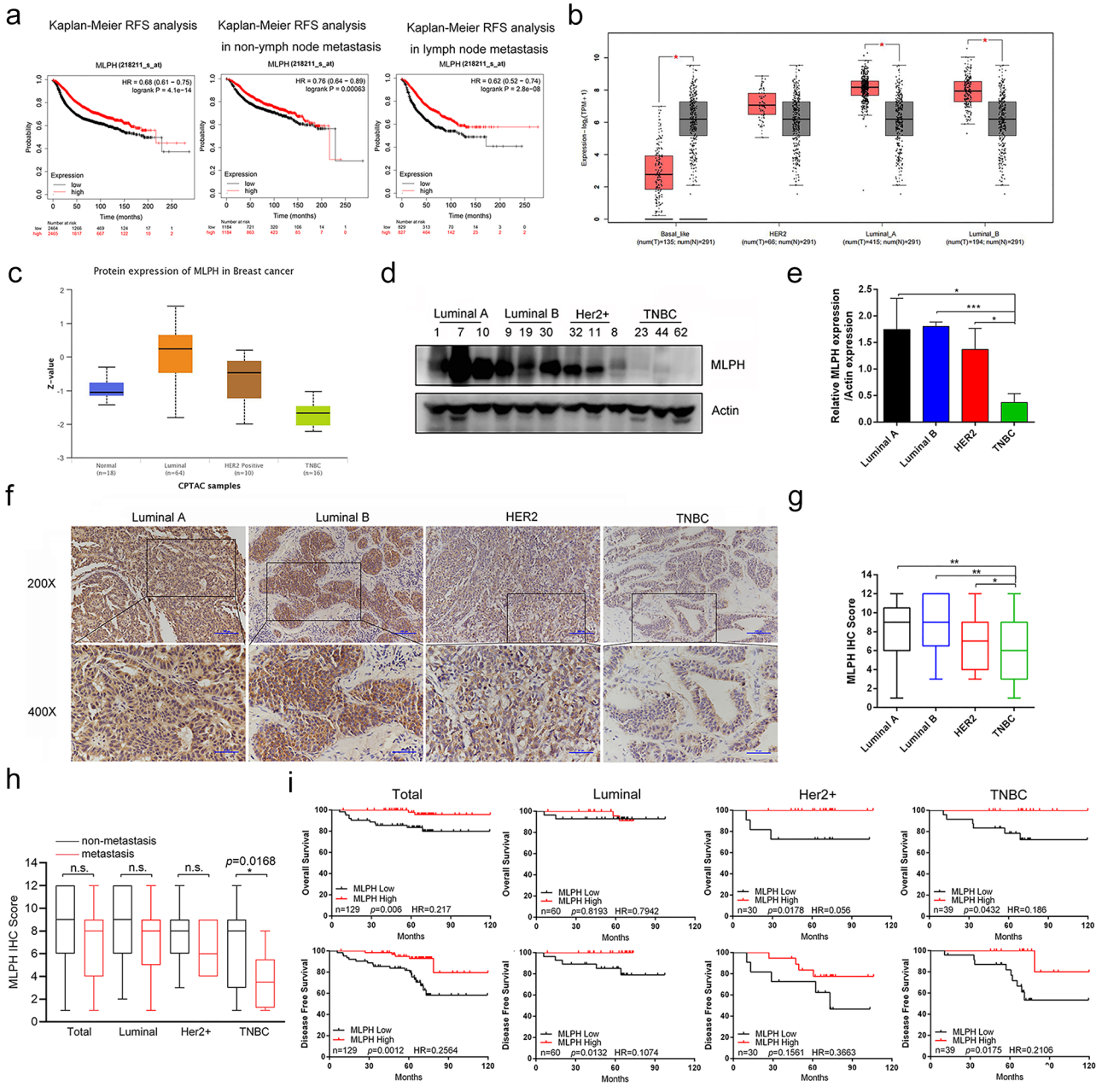

Fig. 2 MLPH is downregulated and negatively correlated with lymph node metastasis in TNBC. **a**. RFS curves for the key gene MLPH of patients with/without lymph node metastasis in the GEO databases. **b**. Predict the expression of MLPH in different subtypes breast cancer and adjacent cancer in TCGA database. **c**. Predict the protein expression of MLPH in different subtypes breast cancer and normal tissues in CPTAC database. **d** and **e**. MLPH expression levels in 80 different subtypes clinical breast tissues were determined by Western blotting with the indicated antibodies. MLPH protein levels were quantified by normalizing to the intensity of the Actin band. Error bars represent the mean ± SEM. $^{*}p < 0.05$, $^{***}p < 0.001$. **f**. Representative images of IHC staining. The boxed areas in the top images are magnified in the bottom images. Original magnification, 100×. **g**. MLPH expression levels in breast cancer tissues. The intensity values in (a) are expressed as the H-score. The relative staining across all samples was shown in the boxplot (t test, $^{*}p < 0.05$, $^{**}p < 0.01$). **h**. MLPH expression levels in different subtypes breast cancer tissues (with and without metastasis). The intensity values in (**a**) are expressed as the H-score. The relative staining across all samples was shown in the boxplot (t-test, $^{*}p < 0.05$). **i**. Kaplan-Meier plot of OS or disease-free survival (DFS) of different subtypes breast cancer patients stratified by MLPH expression levels

assays showed similar results (Fig. 3f). Wound healing and transwell migration and invasion assay showed that directional cell migration toward a "wound" in a cell monolayer was inhibited in MDA-MB-231 cells and HS578T cells stably expressing MLPH (Fig. 3g and h). As shown in Fig. 3i and j, MLPH markedly suppressed the migration and invasion potential of MDA-MB-231 cells and HS578T cells. These findings suggest that MLPH

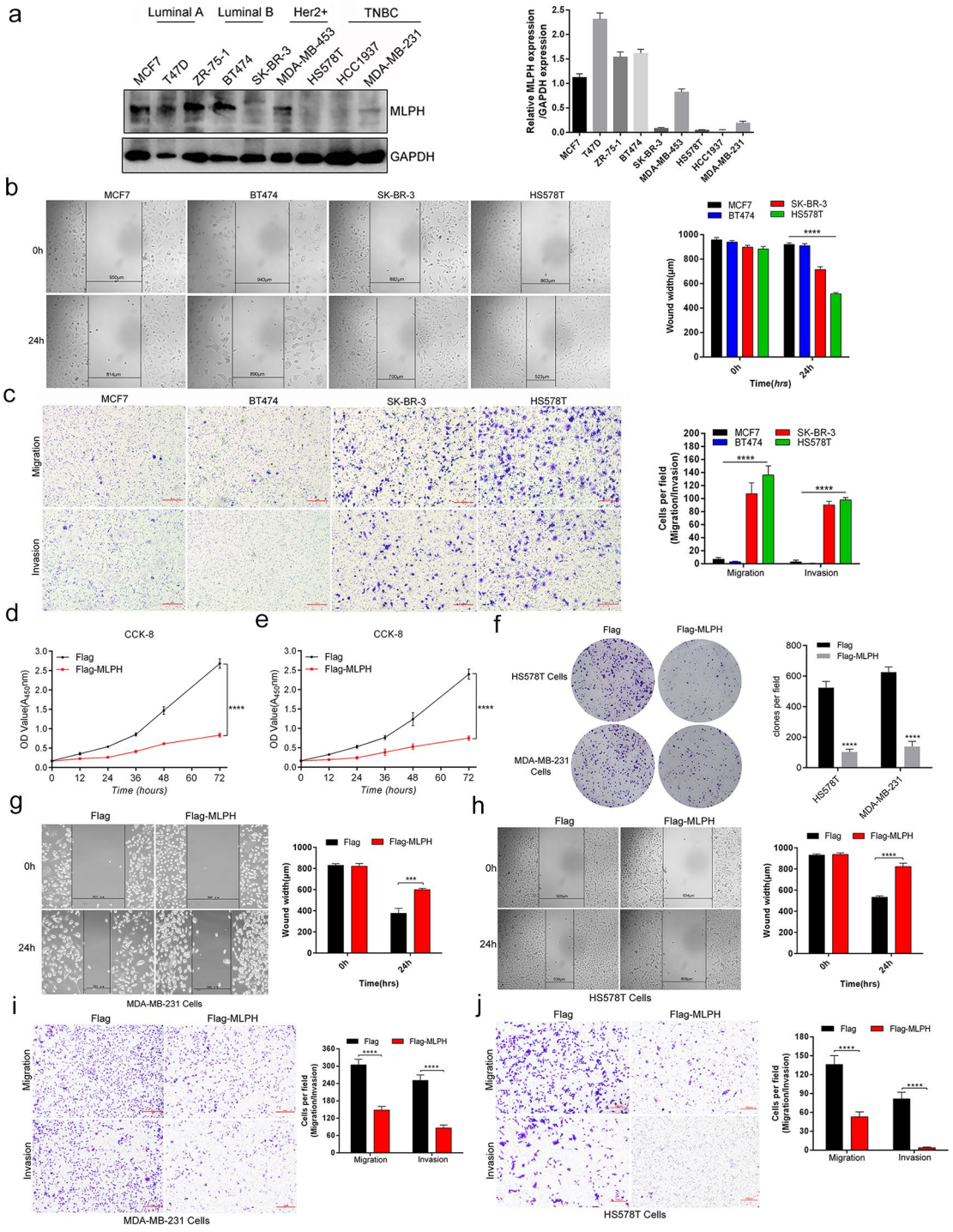

Fig. 3 MLPH inhibits the proliferation, invasion, and migration of TNBC. **a**. The protein expression of MLPH protein was detected in cell lines by western blot. MLPH protein levels were quantified by normalizing to the intensity of the Actin band. Error bars represent the mean ± SEM. $^{*}p < 0.05$, $^{***}p < 0.001$. **b**. Wound-healing analysis of different subtypes breast cancer cells. Results were representative of three independent experiments. $^{****}p < 0.0001$. **c**. Transwell analysis of different subtypes breast cancer cells. Results were representative of three independent experiments. $^{****}p < 0.0001$. **d** and **e**. CCK8 proliferation analysis of HS578T or MDA-MB-231 cells stable transfected with Flag or Flag-MLPH, the data were presented as a histogram of the mean and SEM of three independent experiments, $^{****}p < 0.0001$. **f**. Colony formation analysis of HS578T or MDA-MB-231 cells stable transfected with Flag or Flag-MLPH, representative pictures of the colonies were shown. The data were presented as a histogram of the mean and SEM of three independent experiments. $^{****}p < 0.0001$. **g** and **h**. Wound-healing analysis of MDA-MB-231(**g**) or HS578T(**h**) cells stable transfected with Flag or Flag-MLPH. Results were representative of three independent experiments. $^{***}p < 0.001$, $^{****}p < 0.0001$. **i** and **j**. Transwell analysis of MDA-MB-231(**i**) or HS578T(**j**) cells stable transfected with Flag or Flag-MLPH. Results were representative of three independent experiments. $^{****}p < 0.0001$

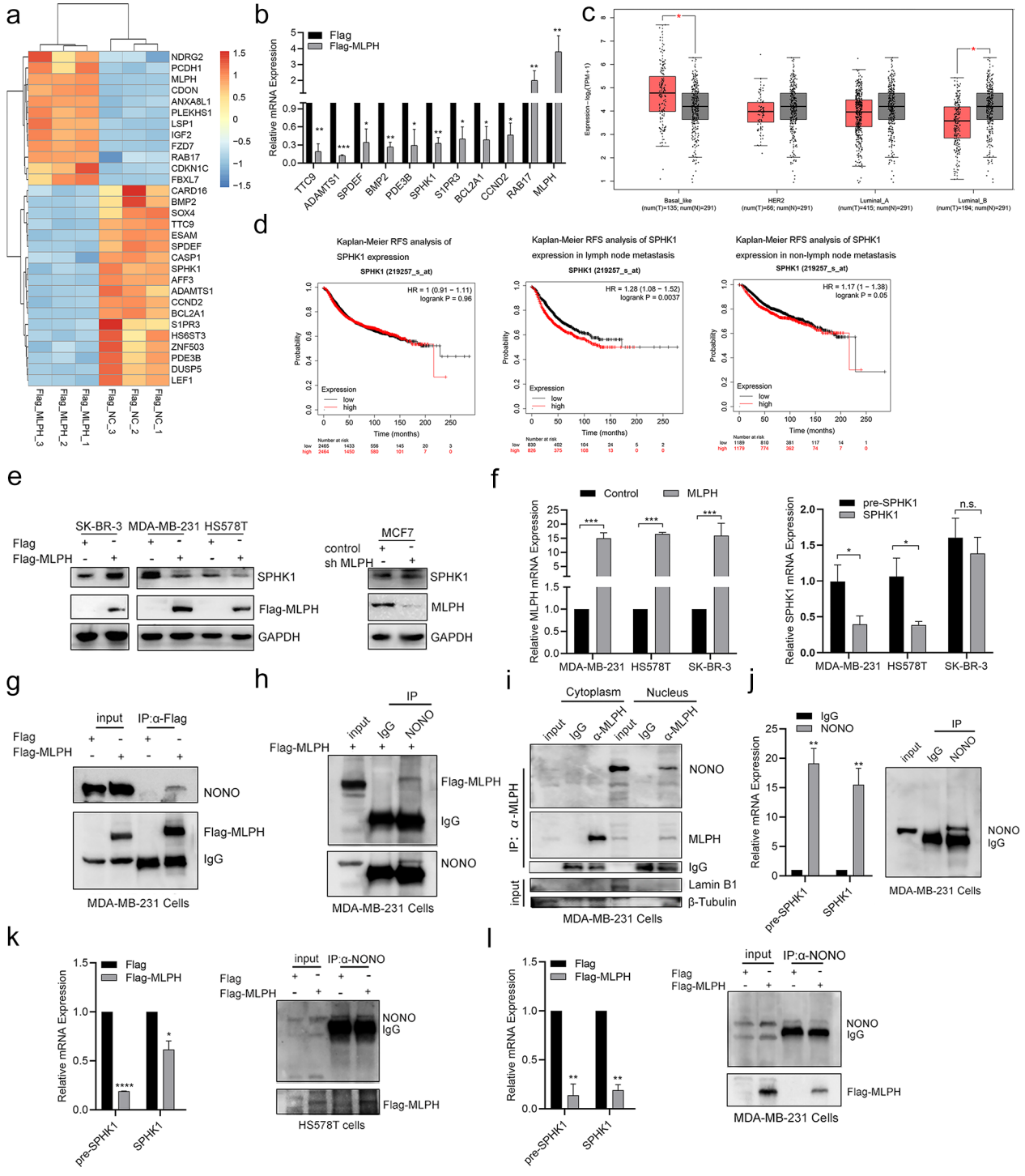

Fig. 4 (See legend on next page.)

inhibits the proliferation, invasion and migration of TNBC cells in vitro.

The mechanism underlying the involvement of MLPH in the progression of TNBC remains unclear. To identify MLPH downstream genes, we performed RNA sequencing (RNA-seq) using MDA-MB-231 cells stably overexpressing MLPH or control cells. RNA-seq analysis and quantitative real-time PCR showed that MLPH downregulates SPHK1, which was thus selected for further analysis (Fig. 4a and b). The expression of SPHK1 in different subtypes of breast cancer was predicted using TCGA and CPTAC databases, and the results showed that SPHK1 is upregulated in TNBC and negatively correlated with the expression of MLPH (Fig. 4c and S3a-3c). SPHK1 was

(See figure on previous page.)

Fig. 4 MLPH prevents the binding of NONO to the SPHK1 pre-RNA to inhibit SPHK1 mRNA splicing in TNBC. **a**. Heatmap analysis of expression differential proteins regulated by MLPH in MDA-MB-231 cells. **b**. qRT-PCR analysis of the expression levels of differential gene in Flag-MLPH overexpressing cells. Levels of all mRNAs were normalized with GAPDH. The data were presented as a histogram of the mean SEM of three independent experiments. Error bars represent mean ± SD. $^{*}p < 0.05$, $^{**}p < 0.01$, $^{***}p < 0.001$, t-test. **c**. Predict the expression of SPHK1 in different subtypes breast cancer and adjacent cancer in TCGA database. **d**. RFS curves for the key gene SPHK1 of patients with/ without lymph node metastasis in the GEO databases. **e**. SK-BR-3, MDA-MB-231 and HS578T cells transfected with Flag or Flag -MLPH; MCF7 cells knock out MLPH, the protein expression was determined by western blotting with the indicated antibodies. **f**. SK-BR-3, MDA-MB-231 and HS578T cells transfected with Flag or Flag -MLPH, qRT-PCR analysis of the expression levels of MLPH, pre-SPHK1, SPHK1. Levels of all mRNAs were normalized with GAPDH. The data were presented as a histogram of the mean SEM of three independent experiments. Error bars represent mean ± SD. $^{*}p < 0.05$, $^{***}p < 0.001$, t-test. **g** and **h**. IP and IB analysis of the interaction of MLPH and NONO in MDA-MB-231 cells. **i**. Separation of cytoplasmic protein and nuclear protein with nucleoplasm separation kit, lysates were subjected to immunoprecipitation and western blot with indicated antibodies. **j**. RIP, qRT-PCR and IB analysis of the interaction of NONO and RNA-SPHK1in MDA-MB-231 cells. **k** and **l**. MDA-MB-231 and HS578T cells transfected with Flag or Flag -MLPH RIP, qRT-PCR and IB analysis of the interaction of NONO and RNA-SPHK1

associated with poor prognosis, and this association was higher in patients with lymph node metastasis (Fig. 4d). To determine whether MLPH regulates the expression of SPHK1, MLPH was overexpressed in SK-BR-3, HS578T, and MDA-MB-231 cells and knocked out MLPH in MCF7 cells. As shown in Fig. 4e and f, MLPH downregulated the protein and mRNA expression, but not the pre-RNA expression of SPHK1 in TNBC (HS578T and MDA-MB-231 cells), whereas this effect was not observed in SK-BR-3 and MCF7 cells. These results indicate that MLPH regulates the expression of SPHK1 at the post-transcriptional level in TNBC cells. The mechanisms underlying the regulation of SPHK1 expression by MLPH were examined by immunoprecipitation (IP) experiments combined with MS-based proteomic analysis to identify potential MLPH-interacting proteins in the MDA-MB-231 cells. MS analyses identified proteins that were specifically associated with MLPH, among which NONO, a member of the human splicing protein family, was selected for further analysis. NONO is a DNA- and RNA-binding protein that participates in various biological events, such as gene transcription regulation, precursor RNA splicing, DNA unwinding and pairing, defective RNA nuclear retention, DNA damage repair, and tumorigenesis (Figure S3d and 3e). We predicted the expression of NONO in different subtypes of breast cancer using TCGA database and found that NONO is upregulated in TNBC (Figure S3f). To validate the MLPH–NONO interaction, we performed a co-immunoprecipitation (co-IP) assay in MDA-MB-231 cells stably transfected with Flag-MLPH. IP with an anti-Flag antibody showed that MLPH interacted with NONO (Fig. 4g), and reciprocal IP with endogenous NONO antibody brought down MLPH (Fig. 4h). The interaction between MLPH and NONO occurred in the nucleus (Fig. 4i). The in vivo association of SPHK1 with NONO was assessed by RNA immunoprecipitation (RIP) and qRT-PCR analysis, which confirmed the binding of NONO to SPHK (Fig. 4j). Finally, we investigated whether MLPH modulates the binding of NONO to SPHK1. RIP and qRT-PCR revealed that MLPH prevents the binding of NONO to SPHK1pre-RNA and mRNA, thereby inhibiting SPHK1 mRNA splicing (Fig. 4k and l). These results indicate that MLPH downregulates the expression of SPHK1 at the post-transcriptional level.

To further examine the role of MLPH in TNBC and to confirm the functional link between MLPH and SPHK1, the protein levels of MLPH and SPHK1 were measured in tumor tissues of different breast cancer subtypes obtained from 50 patients. The results showed that the protein levels of SPHK1 were higher in TNBC than in other breast cancer subtypes (Fig. 5a). Sphingosine-1-phosphate (S1P), the formation of which is catalyzed by SPHK-1 or -2, is a bioactive lipid implicated in human health and disease; it activates signals through the S1P receptor (S1PR) via autocrine or paracrine pathway. S1P expression was measured in different subtypes of breast cancer tissues obtained from 50 breast cancer patients, and the results showed that the levels of S1P were higher in TNBC than in other breast cancer subtypes (Fig. 5b). We next investigated whether MLPH can regulate S1P synthesis. MLPH overexpression decreased the intracellular and extracellular levels of S1P compared with the levels in the control in TNBC (Fig. 5c). These results suggest that MLPH decreases S1P synthesis in TNBC. The effect of MLPH-mediated inhibition of S1P synthesis on tumor growth was examined using the CCK8 assay. HS578T and MDAMB-231 cells stably expressing MLPH showed significantly reduced proliferation in vitro, and addition of S1P reversed the inhibitory effect of MLPH on cell proliferation (Fig. 5d). Colony formation assays showed similar results (Fig. 5e). The role of S1P in cell migration and invasion was examined by wound healing and transwell migration and invasion assays. Overexpression of MLPH strongly inhibited directional cell migration toward a "wound" in a cell monolayer, and treatment with S1P reversed the inhibitory effect of MLPH on cell migration (Fig. 5f and g). As shown in Fig. 5h and i, S1P also reversed the inhibitory effect of MLPH on cell migration and invasion in HS578T and MDAMB-231 cells. Furthermore, Gene Ontology (GO) analysis and Gene Set Enrichment Analysis (GSEA) of the genes associated with MLPH showed that they were mainly involved in cell adhesion (Fig. 5j and k). Overexpression of MLPH

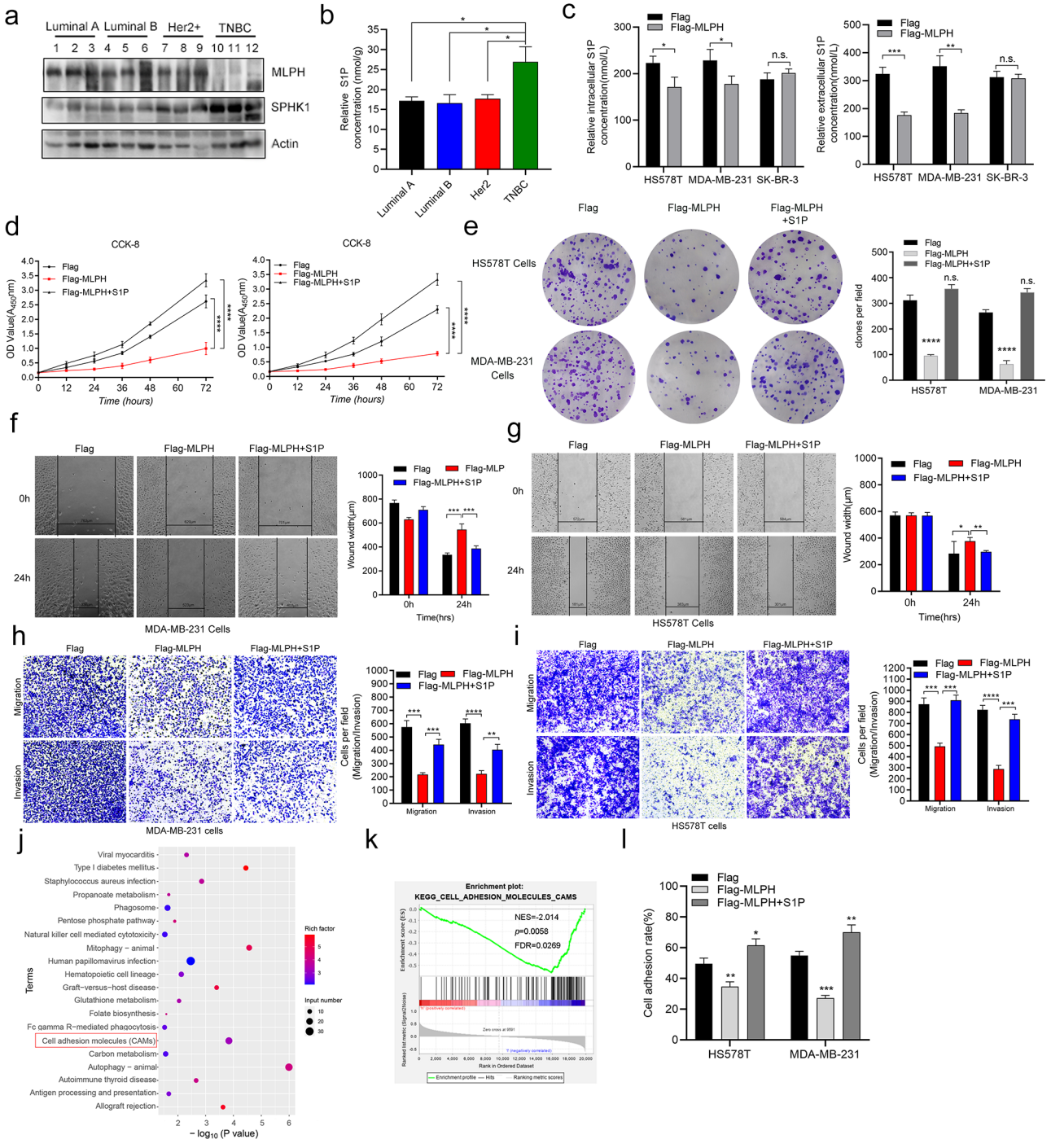

Fig. 5 (See legend on next page.)

strongly inhibited cell adhesion, and adding S1P reversed the inhibitory effect of MLPH on cell adhesion (Fig. 5l). These results suggest that MLPH-mediated inhibition of S1P synthesis suppresses the proliferation, migration, invasion, and adhesion of TNBC cells.

The growth-inhibitory effect of MLPH was tested in vivo in BALB/c female mice subcutaneously injected with 4T1 cells infected with lentiviruses harboring Flag and Flag-MLPH. During tumor formation, mice received daily subcutaneous injections containing S1P (10 mg/kg) in PBS (50 μl) at the periphery of the area of 4T1 cell implantation. At 31 days after cell implantation, subcutaneous nodules became measurable. On day 31 of tumor formation, the mice were euthanized, tumor tissues were excised, weighed, and images were acquired. The results showed that the growth of tumors was significantly

(See figure on previous page.)

Fig. 5 MLPH inhibits cell proliferation, invasion, migration, and adhesion in TNBC through the SPHK1-S1P axis. **a**. MLPH and SPHK1 expression levels in 48 different subtypes clinical breast tissues were determined by Western blotting with the indicated antibodies. **b**. Relative S1P levels of tumor tissues (T). unpaired Student's t-test, $n=48$, $^{*}p<0.05$. **c**. SK-BR-3, MDA-MB-231 and HS578T cells transfected with Flag or Flag -MLPH, and detected the content of intracellular and extracellular S1P. **d**. CCK8 proliferation analysis of HS578T or MDA-MB-231 cells stable transfected with Flag or Flag-MLPH and added S1P (2 μg/ml), the data were presented as a histogram of the mean and SEM of three independent experiments, $^{****}p<0.0001$. **e**. Colony formation analysis of HS578T or MDA-MB-231 cells stable transfected with Flag or Flag-MLPH and added S1P (2 μg/ml), representative pictures of the colonies were shown. The data were presented as a histogram of the mean and SEM of three independent experiments. $^{****}p<0.0001$. **f** and **g**. Wound-healing analysis of MDA-MB-231(g) or HS578T(h) cells stable transfected with Flag or Flag-MLPH and added S1P (2 μg/ml). Results were representative of three independent experiments. $^{*}p<0.05$, $^{**}p<0.01$, $^{***}p<0.001$. **h** and **i**. Transwell analysis of MDA-MB-231(**i**) or HS578T(**j**) cells stable transfected with Flag or Flag-MLPH and added S1P (2 μg/ml). Results were representative of three independent experiments. $^{**}p<0.01$, $^{***}p<0.001$, $^{****}p<0.0001$. **j**. GO analysis of MLPH enriched pathways. **k**. GSEA analysis of MLPH enriched pathways in TCGA databases. **l**. Cell adhesion analysis of HS578T or MDA-MB-231 cells stable transfected with Flag or Flag-MLPH and added S1P (2 μg/ml), the data were presented as a histogram of the mean and SEM of three independent experiments, $^{*}p<0.05$, $^{**}p<0.01$, $^{***}p<0.001$

slower in mice injected with Flag MLPH cells than in the vector group, and injection of S1P reversed the inhibitory effect of MLPH on tumor growth in mice (Fig. 6a and d). Consistently, IHC analyses of SPHK1 revealed significantly lower staining intensity in the MLPH overexpression group than in the controls (Fig. 6e). A significant negative correlation was observed between SPHK1 and MLPH protein levels in mice tumors (Fig. 6f). To examine the role of MLPH in lymph node metastasis, we used the mouse 4T1 cell footpad implantation model. 4T1 cells stably expressing Flag and Flag-MLPH were injected into the footpad of BALB/c mice. S1P (300 mg/kg) in PBS (50 μl) was injected daily subcutaneously into the anterolateral aspect of the mouse leg, above the area of implantation of 4T1 cells in the hind limb foot. The treatment started on week 2 after tumor implantation. Ipsilateral lymph nodes were sampled on day 25 (Fig. 6g). The results showed that lymph node metastasis was markedly lower in mice injected with MLPH stably expressing cells than in the other groups, and S1P treatment reversed the effect of MLPH on lymph node metastasis (Fig. 6h and i). Hematoxylin and eosin staining of the lymph node tumor metastasis area at the study endpoint showed consistent results (Fig. 6j and k). These findings indicate that MLPH inhibits proliferation and lymph node metastasis in TNBC in vivo.

Discussion

TNBC is the most aggressive breast cancer subtype with the worst prognosis, and no targeted treatments are available. TNBC is a heterogeneous disease, and the probability of survival and/or recurrence varies among patients. The rates of metastasis and recurrence are higher in TNBC than in other subtypes of breast cancer [25]. Because metastasis to lymph node is one of the first signs of tumor spread [26, 27], we analyzed gene expression and the clinical characteristics of patients using the GEO TNBC database. We examined the yellow module related to N stage to screen genes related to TNBC and lymph node metastasis, and identified MLPH as a potentially involved gene for further analysis. MLPH is associated with tumor proliferation, metastasis, and postoperative radiotherapy resistance in many cancer types [6, 7, 28, 29]. However, our understanding of the expression and function of MLPH in TNBC remains limited. In this study, we found that although MLPH is expressed at high levels in breast cancer, its expression is lower in TNBC than in other subtypes of breast cancer, suggesting that MLPH plays different roles in different subtypes of breast cancer cells. We analyzed the relationship between MLPH expression and lymph node metastasis in different breast cancer subgroups, and found that MLPH was negatively correlated with lymph node metastasis in TNBC, but not in other breast cancer types. In addition, we demonstrated that overexpression of MLPH in TNBC cells can inhibit cell proliferation, invasion, and migration. However, the specific mechanisms underlying the role of MLPH in regulating proliferation and lymph node metastasis in TNBC need to be further explored.

SPHK was identified as a downstream gene of MLPH by RNA sequencing. Tumor cells express high levels of SPHK1, which acts as a proto-oncogenic factor and is responsible for the synthesis of S1P. S1P functions through either the autocrine or the paracrine pathway and is associated with many process, including anti-apoptotic functions, metastasis, epithelial-mesenchymal transition, angiogenesis, and chemotherapy resistance [30, 31]. Previous studies have demonstrated that metformin, an AMPK activator, affects airway remodeling by inhibiting STAT3 phosphorylation to downregulate the expression of PLK1 and ID2 proteins, thereby inhibiting S1P induced proliferation of airway smooth muscle cells (ASMCs) [32]. S1P participates in the process of bile stasis by activating S1PRs. Mice primary hepatocytes treated with SEW2871 (S1P agonist) increased the expression of S1PR1 and activated AMPK which effectively improved α-naphthalene isothiocyanate (ANIT) induced cholestatic liver injury [33]. These studies indicate that the AMPK signaling pathway is the downstream of the S1P-S1PRs axis.

Due to the significant inhibition of the tumor proliferation by AMPK activators, multiple clinical trials have been conducted on the combination of AMPK activators and rapamycin in treatment of leukemia [34]. In

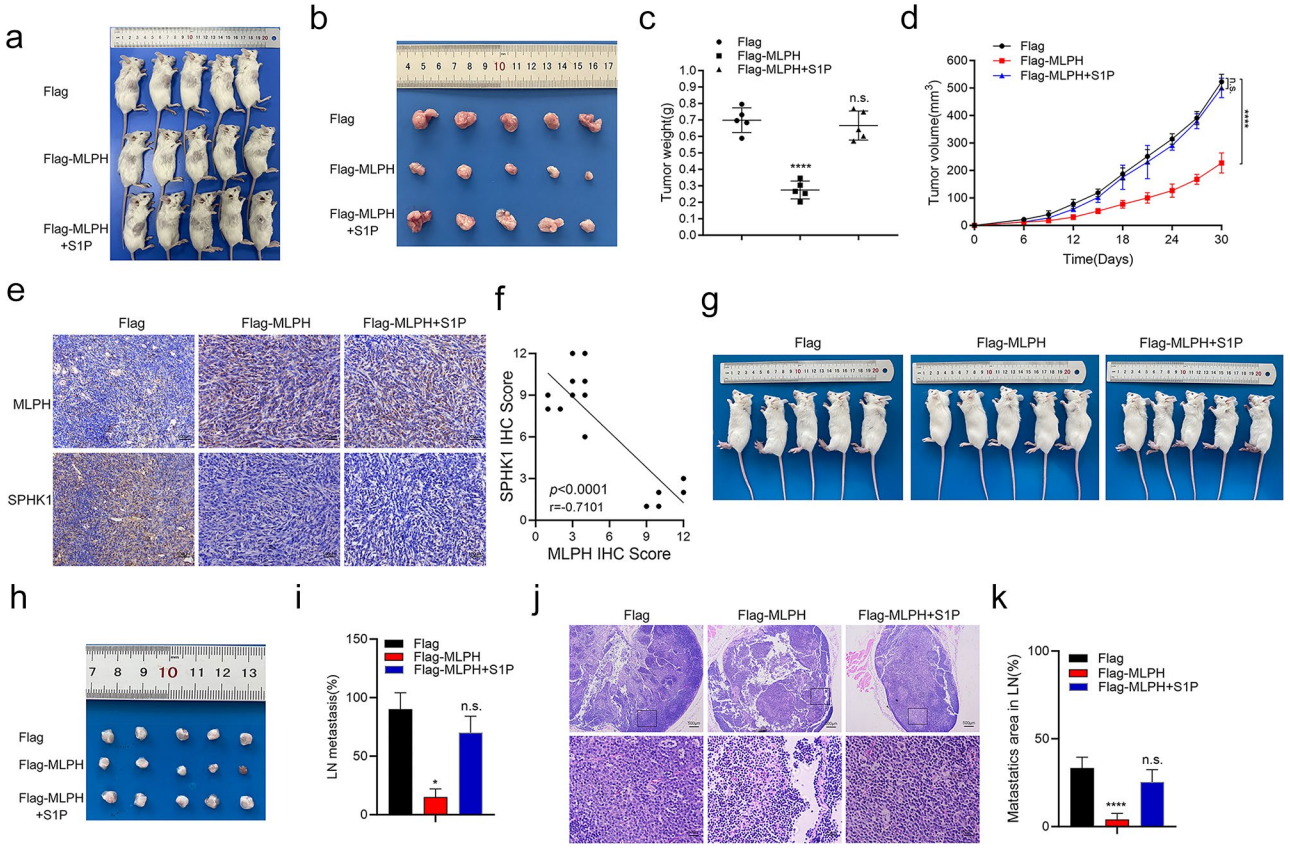

Fig. 6 MLPH inhibits proliferation and lymph node metastasis in TNBC *in vivo*. **a**. Representative mice with subcutaneously injected 4T-1 stably transfected cells. **b**. Representative tumor from Flag and Flag-MLPH 4T1 cells. **c**. Quantitation of tumor weights was presented as a histogram (5 mice per group. $^{****}p < 0.0001$). **d**. Tumor diameter was measured at the indicated time points, and tumor volume was calculated. The results were presented as the mean and SEM of 5 mice per group per time point, $^{****}p < 0.0001$. **e**. Representative images of IHC staining showing MLPH and SPHK1 protein expression in each group mice's tumors. **f**. Pearson correlation analysis of PAK5 and HMGCS2 protein expression levels, $^{****}p < 0.0001$. **g**. Representative mice with subcutaneously injected 4T-1 stably transfected cells. **h** and **i**. Comparison of the gross appearances of metastatic pLNs and various metastasis parameters between Flag, Flag-MLPH and Flag-MLPH + S1P groups ($n = 5$ samples for each group), $^{*}p < 0.05$, Error bars are presented as mean ± SEM. **j**. Representative images of HE and IHC staining showing metastatic pLNs and highly magnified tumor margins. The boxed areas in the top images are magnified in the bottom images. Original magnification, 100×. **k**. Comparison of transfer regions in transferable pLNs. $^{****}p < 0.0001$, Error bars are presented as mean ± SEM

breast cancer, metformin, commonly used to treat type 2 diabetes, has revealed potential benefits in both observational and preclinical studies across breast cancer subtypes [35]. Another AMPK activator, 5-aminoimidazole-4-formamide ribonucleotides (AICAR), inhibited tumor growth, migration and invasion of TNBC cells [36]. Furthermore, previous study has demonstrated that AICAR enhanced the efficacy of rapamycin by inhibiting mTORC1 [37]. However, the concentration of rapamycin used to treated TNBC was much higher that of other types of breast cancer, which indicated that the combination strategy was not satisfactory. Therefore, it is particularly important to find a new target for TNBC treatment.

In this study, we found that MLPH downregulates the expression of SPHK1 at the mRNA and protein levels, but not the pre-RNA expression in TNBC. However, this regulation regulatory role was not observed in other subtypes of breast cancer. These results suggest that MLPH decreases the synthesis of S1P to inhibit cell adhesion by regulating the expression of SPHK1 at the post-transcriptional level, thereby inhibiting growth and lymph node metastasis in TNBC.

mRNA splicing is a critical step in post-transcriptional gene regulation, and it expands the functional proteome in eukaryotes. We identified the RNA binding protein NONO as a protein specifically associated with MLPH by MS analysis. NONO interacts with the m6A reader IGF2BP3 to promote DLG1 RNA splicing, which increases the growth of gallbladder cancer [38]. NONO regulates mRNA splicing in glioblastoma, and knockdown of NONO impairs tumor growth, invasion, and redox homeostasis by leading to aberrant splicing of GPX1 [21]. NONO interacts directly with splicing factor proline/glutamine rich to regulate the splicing of SETMAR, suppressing metastasis in bladder cancer [39]. In this study, we demonstrated that NONO binds to the

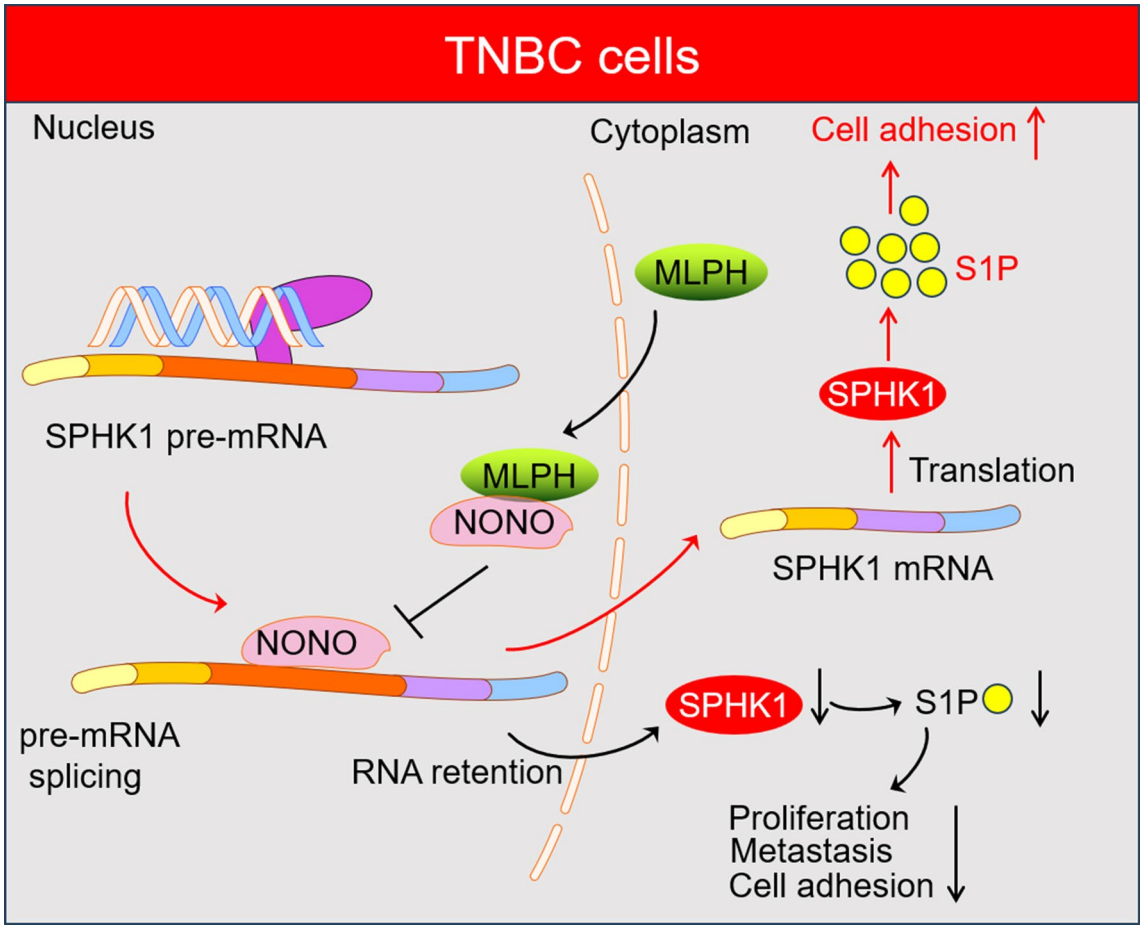

Fig. 7 The mechanisms of MLPH in controlling proliferation and lymph node metastasis in TNBC. In TNBC cells, MLPH is lower expression than other subtypes of breast cancer cells. NONO is identified as an essential factor involved in SPHK1 mRNA splicing. Ectopic overexpression of MLPH interacts with NONO to inhibit mRNA splicing of SPHK1, which reduces the content of S1P, thereby inhibiting growth and lymph node metastasis in TNBC

pre-RNA of SPHK1, and MLPH prevents this binding to inhibit SPHK1 mRNA splicing in TNBC.

The functions of S1P varies depending on the cancer types, subtypes, progression, and tumor microenvironment [40, 41]. In addition to treatment with anti-S1P antibodies targeting S1P itself, treatment with antagonist of S1P receptors and S1P-producing enzymes inhibitors are being considered for targeting the S1P signaling pathway, and new drugs are being developed [42–44]. FTY720 (Fingomode) has been shown to inhibit S1P receptors other than S1PR2, as well as SPHK1 in the basic study is the first molecular targeted drug approved for multiple sclerosis. However, due to the immunosuppressive side effects of FTY720, its clinical application as an anti-cancer drug has not yet made progress [45–49]. We found that MLPH expression in TNBC is low. MLPH inhibited the tumor growth and lymph node metastasis of TNBC through the NONO-SPHK1-S1P signaling pathway. MLPH may be a new target of TNBC for S1P signal transduction therapy.

In conclusion, we elucidated a mechanism underlying lymph node metastasis in TNBC and identified the role of the MLPH-NONO-SPHK1-S1P axis in regulating proliferation and lymph node metastasis in TNBC (Fig. 7). These findings may help design strategies for predicting and treating metastasis in TNBC.

Supplementary Information

The online version contains supplementary material available at https://doi.org/10.1186/s12967-025-06240-9.

Supplementary Material 1

Supplementary Material 2

Supplementary Material 3

Supplementary Material 4

Author contributions

Yao Xing and Shulan Sun designed experiments. Yao Xing, Yuen Tan, and Qingchuan Chen performed experiments. Yefu Liu collected patient samples that were stained for MLPH, which were analyzed by Yuen Tan and Jianjun Zhang. Yefu Liu provided clinical data and critical input. Yao Xing wrote the paper. Jianjun Zhang, Yefu Liu, and Shulan Sun supervised the study. Yao Xing,

Yuen Tan and Shulan Sun contributed to funding acquisition. All authors have read and agreed to the published version of the manuscript.

Funding
This work was supported by National Science Foundation of China Grants (Nos. 82203830 and 82303492). Project of science and Technology Department of Liaoning Province [2023-MSLH-160 and 2022-BS-062]. The Outstanding Youth Foundation of Liaoning (No. 2022-YQ-08). The Liaoning Provincial Key Laboratory of Precision Medicine for Malignant Tumors (Project number: 220569).

Data availability
The data that support the findings of this study are available from the corresponding author upon reasonable request.

Declarations

Ethical approval
The authors are accountable for all aspects of the work in ensuring that questions related to the accuracy or integrity of any part of the work are appropriately investigated and resolved. This study was approved by Ethics Committee of the Cancer Hospital of China Medical University (ID: KY20230719). Informed consent was obtained from each participant. The study was conducted in accordance with the Declaration of Helsinki (as revised in 2013). The animal research protocol was approved by the Animal Center of China Medical University, in compliance with institutional guidelines for the care and use of animals.

Competing interests
The authors declare no competing interests.

Received: 11 November 2024 / Accepted: 11 February 2025
Published online: 06 March 2025

References

1. Bray F, Laversanne M, Sung H, Ferlay J, Siegel RL, Soerjomataram I, Jemal A. Global cancer statistics 2022: GLOBOCAN estimates of incidence and mortality worldwide for 36 cancers in 185 countries. Cancer J Clin. 2024;74:229–63.
2. Leon-Ferre RA, Goetz MP. Advances in systemic therapies for triple negative breast cancer. BMJ (Clinical Res ed). 2023;381:e071674.
3. Li Y, Zhang H, Merkher Y, Chen L, Liu N, Leonov S, Chen Y. Recent advances in therapeutic strategies for triple-negative breast cancer. J Hematol Oncol. 2022;15:121.
4. Barral DC, Seabra MC. The melanosome as a model to study organelle motility in mammals. Pigment Cell Res. 2004;17:111–8.
5. Lee JA, Hwang SJ, Hong SC, Myung CH, Lee JE, Park JI, Hwang JS. Identification of MicroRNA Targeting Mlph and Affecting Melanosome Transport. Biomolecules. 2019;9.
6. Li W-S, Chen C-I, Chen H-P, Liu K-W, Tsai C-J, Yang C-C. Overexpression of MLPH in Rectal Cancer Patients Correlates with a Poorer Response to Preoperative Chemoradiotherapy and Reduced Patient Survival. Diagnostics (Basel, Switzerland). 2021;11.
7. Xu L, Ye Y, Tao Z, Wang T, Wei Y, Cai W, Wan X, Zhao P, Gu W, Gu B, Zhang L, Tian Y, Liu N, et al. O-GlcNAcylation of melanophilin enhances radiation resistance in glioblastoma via suppressing TRIM21 mediated ubiquitination. Oncogene. 2024;43:61–75.
8. Ogretmen B. Sphingolipid metabolism in cancer signalling and therapy. Nat Rev Cancer. 2018;18:33–50.
9. Pyne NJ, Pyne S. Sphingosine 1-phosphate and cancer. Nat Rev Cancer. 2010;10:489–503.
10. Kawai H, Osawa Y, Matsuda M, Tsunoda T, Yanagida K, Hishikawa D, Okawara M, Sakamoto Y, Shimagaki T, Tsutsui Y, Yoshida Y, Yoshikawa S, Hashi K, et al. Sphingosine-1-phosphate promotes tumor development and liver fibrosis in mouse model of congestive hepatopathy. Hepatology (Baltimore MD). 2022;76:112–25.
11. Hait NC, Allegood J, Maceyka M, Strub GM, Harikumar KB, Singh SK, Luo C, Marmorstein R, Kordula T, Milstien S, Spiegel S. Regulation of histone acetylation in the nucleus by sphingosine-1-phosphate. Volume 325. New York, NY): Science; 2009. pp. 1254–7.
12. Kwong EK, Li X, Hylemon PB, Zhou H. Sphingosine Kinases/Sphingosine 1-Phosphate signaling in hepatic lipid metabolism. Curr Pharmacol Rep. 2017;3:176–83.
13. Maiti A, Takabe K, Hait NC. Metastatic triple-negative breast cancer is dependent on SphKs/S1P signaling for growth and survival. Cell Signal. 2017;32:85–92.
14. Sukocheva OA, Hu DG, Meech R, Bishayee A. Divergence of Intracellular Trafficking of Sphingosine Kinase 1 and sphingosine-1-Phosphate receptor 3 in MCF-7 breast Cancer cells and MCF-7-Derived stem cell-enriched mammospheres. Int J Mol Sci. 2021;22.
15. Nagahashi M, Ramachandran S, Kim EY, Allegood JC, Rashid OM, Yamada A, Zhao R, Milstien S, Zhou H, Spiegel S, Takabe K. Sphingosine-1-phosphate produced by sphingosine kinase 1 promotes breast cancer progression by stimulating angiogenesis and lymphangiogenesis. Cancer Res. 2012;72:726–35.
16. Bentley DL. Coupling mRNA processing with transcription in time and space. Nat Rev Genet. 2014;15:163–75.
17. Qin H, Ni H, Liu Y, Yuan Y, Xi T, Li X, Zheng L. RNA-binding proteins in tumor progression. J Hematol Oncol. 2020;13:90.
18. Jaafar L, Li Z, Li S, Dynan WS. SFPQ•NONO and XLF function separately and together to promote DNA double-strand break repair via canonical nonhomologous end joining. Nucleic Acids Res. 2017;45:1848–59.
19. Dong X, Sweet J, Challis JRG, Brown T, Lye SJ. Transcriptional activity of androgen receptor is modulated by two RNA splicing factors, PSF and p54nrb. Mol Cell Biol. 2007;27:4863–75.
20. Li H, Jiao W, Song J, Wang J, Chen G, Li D, Wang X, Bao B, Du X, Cheng Y, Yang C, Tong Q, Zheng L. circ-hnRNPU inhibits NONO-mediated c-Myc transactivation and mRNA stabilization essential for glycosylation and cancer progression. J Experimental Clin Cancer Research: CR. 2023;42:313.
21. Wang X, Han M, Wang S, Sun Y, Zhao W, Xue Z, Liang X, Huang B, Li G, Chen A, Li X, Wang J. Targeting the splicing factor NONO inhibits GBM progression through GPX1 intron retention. Theranostics. 2022;12:5451–69.
22. Shen M, Zhang R, Jia W, Zhu Z, Zhao L, Huang G, Liu J. RNA-binding protein p54nrb/NONO potentiates nuclear EGFR-mediated tumorigenesis of triple-negative breast cancer. Cell Death Dis. 2022;13:42.
23. Kim S-J, Ju J-S, Kang M-H, Eun JW, Kim YH, Raninga PV, Khanna KK, Győrffy B, Pack C-G, Han H-D, Lee HJ, Gong G, Shin Y, et al. RNA-binding protein NONO contributes to cancer cell growth and confers drug resistance as a theranostic target in TNBC. Theranostics. 2020;10:7974–92.
24. Li Y, Xing Y, Wang X, Hu B, Zhao X, Zhang H, Han F, Geng N, Wang F, Li Y, Li J, Jin F, Li F. PAK5 promotes RNA helicase DDX5 sumoylation and miRNA-10b processing in a kinase-dependent manner in breast cancer. Cell Rep. 2021;37:110127.
25. Loibl S, Poortmans P, Morrow M, Denkert C, Curigliano G. Breast cancer. Lancet (London England). 2021;397:1750–69.
26. Min SK, Lee SK, Woo J, Jung SM, Ryu JM, Yu J, Lee JE, Kim SW, Chae BJ, Nam SJ. Relation between tumor size and Lymph Node Metastasis according to subtypes of breast Cancer. J Breast Cancer. 2021;24:75–84.
27. Martínez-Gregorio H, Rojas-Jiménez E, Mejía-Gómez JC, Díaz-Velásquez C, Quezada-Urban R, Vallejo-Lecuona F, de la Cruz-Montoya A, Porras-Reyes FI, Pérez-Sánchez VM, Maldonado-Martínez HA, Robles-Estrada M, Bargalló-Rocha E, Cabrera-Galeana P et al. The evolution of clinically aggressive triple-negative breast Cancer shows a large mutational diversity and early metastasis to Lymph Nodes. Cancers. 2021;13.
28. Jiang C, Wu S, Jiang L, Gao Z, Li X, Duan Y, Li N, Sun T. Network-based approach to identify biomarkers predicting response and prognosis for HER2-negative breast cancer treatment with taxane-anthracycline neoadjuvant chemotherapy. PeerJ. 2019;7:e7515.
29. Liu J, Chang X, Qian L, Chen S, Xue Z, Wu J, Luo D, Huang B, Fan J, Guo T, Nie X. Proteomics-Derived Biomarker Panel Facilitates Distinguishing Primary Lung Adenocarcinomas With Intestinal or Mucinous Differentiation From Lung Metastatic Colorectal Cancer. Molecular & Cellular Proteomics: MCP. 2024;23:100766.
30. Rostami N, Nikkhoo A, Ajjoolabady A, Azizi G, Hojjat-Farsangi M, Ghalamfarsa G, Yousefi B, Yousefi M, Jadidi-Niaragh F. S1PR1 as a Novel Promising Therapeutic Target in Cancer Therapy. Mol Diagn Ther. 2019;23:467–87.
31. Riboni L, Abdel Hadi L, Navone SE, Guarnaccia L, Campanella R, Marfia G. Sphingosine-1-Phosphate in the Tumor Microenvironment: A Signaling Hub Regulating Cancer Hallmarks. Cells. 2020;9.
32. Pan Y, Liu L, Zhang Q, Shi W, Feng W, Wang J, Wang Q, Li S, Li M. Activation of AMPK suppresses S1P-induced airway smooth muscle cells proliferation and its potential mechanisms. Mol Immunol. 2020;128:106–15.

33. Yang T, Wang X, Zhou Y, Yu Q, Heng C, Yang H, Yuan Z, Miao Y, Chai Y, Wu Z, Sun L, Huang X, Liu B, et al. SEW2871 attenuates ANIT-induced hepatotoxicity by protecting liver barrier function via sphingosine 1-phosphate receptor-1-mediated AMPK signaling pathway. Cell Biol Toxicol. 2021;37:595–609.
34. Sengupta TK, Leclerc GM, Hsieh-Kinser TT, Leclerc GJ, Singh I, Barredo JC. Cytotoxic effect of 5-aminoimidazole-4-carboxamide-1-beta-4-ribofuranoside (AICAR) on childhood acute lymphoblastic leukemia (ALL) cells: implication for targeted therapy. Mol Cancer. 2007;6:46.
35. Goodwin PJ, Chen BE, Gelmon KA, Whelan TJ, Ennis M, Lemieux J, Ligibel JA, Hershman DL, Mayer IA, Hobday TJ, Bliss JM, Rastogi P, Rabaglio-Poretti M, et al. Effect of Metformin vs Placebo on Invasive Disease-Free Survival in patients with breast Cancer: the MA.32 Randomized Clinical Trial. JAMA. 2022;327:1963–73.
36. Gollavilli PN, Kanugula AK, Koyyada R, Karnewar S, Neeli PK, Kotamraju S. AMPK inhibits MTDH expression via GSK3β and SIRT1 activation: potential role in triple negative breast cancer cell proliferation. FEBS J. 2015;282:3971–85.
37. Mukhopadhyay S, Chatterjee A, Kogan D, Patel D, Foster DA. 5-Aminoimidazole-4-carboxamide-1-β-4-ribofuranoside (AICAR) enhances the efficacy of rapamycin in human cancer cells. Cell Cycle (Georgetown Tex). 2015;14:3331–9.
38. Yang Z-Y, Zhao C, Liu S-L, Pan L-J, Zhu Y-d, Zhao J-W, Wang H-K, Ye Y-Y, Qiang J, Shi L-Q, Mei J-W, Xie Y, Gong W, et al. NONO promotes gallbladder cancer cell proliferation by enhancing oncogenic RNA splicing of DLG1 through interaction with IGF2BP3/RBM14. Cancer Lett. 2024;587:216703.
39. Xie R, Chen X, Cheng L, Huang M, Zhou Q, Zhang J, Chen Y, Peng S, Chen Z, Dong W, Huang J, Lin T. NONO inhibits lymphatic metastasis of bladder Cancer via Alternative Splicing of SETMAR. Mol Therapy: J Am Soc Gene Therapy. 2021;29:291–307.
40. Di Paolo A, Vignini A, Alia S, Membrino V, Delli Carpini G, Giannella L, Ciavattini A. Pathogenic role of the sphingosine 1-Phosphate (S1P) pathway in Common Gynecologic disorders (GDs): a possible Novel Therapeutic Target. Int J Mol Sci. 2022;23.
41. Chen H, Wang J, Zhang C, Ding P, Tian S, Chen J, Ji G, Wu T. Sphingosine 1-phosphate receptor, a new therapeutic direction in different diseases. Volume 153. Biomedicine & Pharmacotherapy = Biomedecine & Pharmacotherapie; 2022. p. 113341.
42. Visentin B, Vekich JA, Sibbald BJ, Cavalli AL, Moreno KM, Matteo RG, Garland WA, Lu Y, Yu S, Hall HS, Kundra V, Mills GB, Sabbadini RA. Validation of an anti-sphingosine-1-phosphate antibody as a potential therapeutic in reducing growth, invasion, and angiogenesis in multiple tumor lineages. Cancer Cell. 2006;9:225–38.
43. Sabbadini RA. Sphingosine-1-phosphate antibodies as potential agents in the treatment of cancer and age-related macular degeneration. Br J Pharmacol. 2011;162:1225–38.
44. Tsuchida J, Nagahashi M, Takabe K, Wakai T. Clinical Impact of Sphingosine-1-Phosphate in Breast Cancer. Mediators of Inflammation. 2017;2017:2076239.
45. Brinkmann V, Billich A, Baumruker T, Heining P, Schmouder R, Francis G, Aradhye S, Burtin P. Fingolimod (FTY720): discovery and development of an oral drug to treat multiple sclerosis. Nat Rev Drug Discovery. 2010;9:883–97.
46. Hait NC, Avni D, Yamada A, Nagahashi M, Aoyagi T, Aoki H, Dumur CI, Zelenko Z, Gallagher EJ, Leroith D, Milstien S, Takabe K, Spiegel S. The phosphorylated prodrug FTY720 is a histone deacetylase inhibitor that reactivates ERα expression and enhances hormonal therapy for breast cancer. Oncogenesis. 2015;4:e156.
47. Kolodziej MA, Al Barim B, Nagl J, Weigand MA, Uhl E, Uhle F, Di Fazio P, Schwarm FP, Stein M. Sphingosine–1–phosphate analogue FTY720 exhibits a potent anti–proliferative effect on glioblastoma cells. Int J Oncol. 2020;57:1039–46.
48. Gupta P, Taiyab A, Hussain A, Alajmi MF, Islam A, Hassan MI. Targeting the Sphingosine Kinase/Sphingosine-1-Phosphate Signaling Axis in Drug Discovery for Cancer Therapy. Cancers. 2021;13.
49. Nagahashi M, Miyoshi Y. Targeting Sphingosine-1-Phosphate signaling in breast Cancer. Int J Mol Sci. 2024;25.

Publisher's note